J Mol Model (2013) 19:263–274
DOI 10.1007/s00894-012-1544-7

ORIGINAL PAPER

Probing the structural and electronic properties of aluminum-sulfur Al_nS_m ($2 \le n+m \le 6$) clusters and their oxides

Ming-Min Zhong · Xiao-Yu Kuang · Zhen-Hua Wang · Peng Shao · Li-Ping Ding

Received: 21 May 2012 / Accepted: 23 July 2012 / Published online: 8 August 2012

Abstract Using the first-principle density functional calculations, the equilibrium geometries and electronic properties of anionic and neutral aluminum-sulfur Al_nS_m ($2 \le n+m \le 6$) clusters have been systematically investigated at B3PW91 level. The optimized results indicate that the lowest-energy structures of the anionic and neutral Al_nS_m clusters prefer the low spin multiplicities (singlet or doublet) except the Al_2^-, Al_2, S_2, Al_4 and Al_2S_4 clusters. A significant odd-even oscillation of the highest occupied-lowest unoccupied molecular orbital (HOMO-LUMO) energy gaps for the $Al_nS_m^-$ clusters is observed. Electron detachment energies (both vertical and adiabatic) are discussed and compared with the photoelectron spectra observations. Furthermore, a good agreement between experimental and theoretical results gives confidence in the most stable clusters considered in the present study and validates the chosen computational method. In addition, the variation trend of chemical hardness is in keeping with that of HOMO-LUMO energy gaps for the Al_nS_m clusters. Upon the interaction of oxygen with the stable AlS_m^- clusters, the dissociative chemisorptions are favorable in energy. The binding energy and Gibbs free energy change show completely opposite oscillating behaviors as the cluster size increases.

Keywords Aluminum-sulfur cluster · Density functional theory · Photoelectron spectrum · Electronic property

Introduction

Elemental sulfur not only has the largest number of allotropes of any element in the periodic table, but is also one of most widely used nonmetallic minerals. It plays an important role in biology, chemistry, industry, pharmacy and several other scientific disciplines as well as being a material of obvious importance to many aspects of daily life [1]. The interaction of sulfur with aluminum is a universal reaction, and aluminum sulfides are extraordinary important industrial materials that have many technological applications. Understanding the mechanism of sulfur atoms reacting with aluminum is deeply meaningful because it can provide a molecular-level understanding in many research fields such as surface and catalysis related to aluminum [2]. So, our current study focuses on the physical origin of the electronic properties of the small mixed aluminum-sulfur clusters, and these properties are of increasing sensitivity in the cluster structure and bonding.

In the last decades, clusters of two elements have attracted much attention because of their variety of electronic and geometric characteristics. Among them, metal sulfides have been extensively investigated from the viewpoint of synthetic organometallic compounds [3], superconductors [4, 5], biochemical systems [6], and catalytic processes [7], since the novel properties and comprehensive technical applications of the metal sulfides. Many experimental techniques, such as Fourier-transform ion cyclotron resonance mass spectrometry (FTICR-MS) [8–13], anion photoelectron spectroscopy (PES) [14–19] and reflection time of flight mass spectrometer (PTOF-MS) [20–23] have been used to study the metal sulfide systems. Dance and co-workers generated many transition-metal sulfides using the laser ablation method and analyzed them by FTICR-MS [8–13]. Meanwhile, Nakajima and co-worker performed a systematic investigation about the anion PES of the aluminum-, iron-, and manganese-sulfur clusters [14–18]. Subsequently, manganese polysulfide cations MnS_x^+ (x=1–10) were studied with mass-selected photodissociation experiments by Zhao et al. [23], who found that MnS^+,

M.-M. Zhong · X.-Y. Kuang (✉) · Z.-H. Wang · P. Shao · L.-P. Ding
Institute of Atomic and Molecular Physics, Sichuan University, Chengdu 610065, China
e-mail: scu_kuang@163.com

MnS_2^+ and MnS_3^+ undergo dissociation at 355 nm by loss of S, S_2 and S_3, respectively. On the theoretical side, density functional theory (DFT) has been regarded as an effective method to simulate the chemical systems because it can accurately estimate the physicochemical properties of clusters with less computational effort. The magnetic and electronic structures of the Fe-S clusters in both synthetic analogues and proteins were interrogated using broken-symmetry DFT [24–27]. Liang et al. investigated the sulfides of group 4–6, 8 and 10 transition metals using DFT calculations and compared with matrix-isolation infrared spectroscopy experiment results [28–32]. Unfortunately, to the best of our knowledge, there have been relatively few systematical investigations of the aluminum-sulfur clusters. Even the electronic structure of the simplest AlS diatomic molecule is still not well understood. Nevertheless, it is highly important to understand the intrinsic electronic structure and chemical bonding in the diatomic Al-S clusters. What kind of regular changes exist in serial Al_nS_m clusters?

In the current work, we are interested in probing the electronic structure and chemical bonding of broad range for aluminum-sulfur systems. The evolutions of geometric structures and electronic properties of mixed anionic and neutral Al_nS_m clusters have been systematically investigated by using the first-principle method based on DFT. Some interesting periodic tends for structural properties, HOMO-LUMO energy gaps and chemical hardness are observed for the anionic and neutral Al_nS_m clusters. A significant odd-even oscillation of the HOMO-LUMO energy gaps for the $Al_nS_m^-$ clusters is observed. Moreover, the calculated VDE and ADE results are in good agreement with the previously published photoelectron spectra results. It is hoped that our theoretical study not only would be useful in deeply understanding the influence of local structure on material's properties, but also can provide powerful guidelines for future experimental research.

Computational methods

Geometric and electronic structures, together with the frequency analysis of the anionic and neutral Al_nS_m clusters and $AlS_mO_2^-$ cluster complexes were determined by means of generalized gradient approximation to DFT using *GAUSSIAN 03* programs [33]. B3PW91, Becke's three parameters hybrid functional [34] combined with Perdew-Wang's correlation functional [35] was employed in this calculation, which has been used successfully for metal sulfides based on recent literature [31, 32]. The standard all-electron 6-311+G (3df) basis set was adopted for the Al, S and O atoms. A strict convergence criterion was used for the total energy, minimized up to 10^{-8} au. The most stable structures of both anionic and neutral Al_nS_m clusters were obtained by carrying out geometry optimization of various structural isomers without any symmetry constraints. The configurations were regarded as optimized when the maximum force, the root-mean-square (RMS) force, the maximum displacement of atoms, and the RMS displacement of atoms had magnitudes less than 0.00045, 0.0003, 0.0018 and 0.0012 au, respectively. Different possible spin multiplicities were also considered for each of these structural isomers to determine the preferred spin states. Spin-restricted hybrid DFT calculations were employed for the singlet state, while spin-unrestricted hybrid DFT calculations were employed for all other electronic states. In addition, vibrational frequency calculations were performed to ascertain the stability of lowest-energy isomers. Thus, the reported states in Figs. 1 and 2 were true local minima since they had real frequencies. Moreover, reliability of the present computational method was validated by performing calculation on the vertical detachment energies (VDE) and adiabatic detachment energies (ADE), for which experimental results are available.

Results and discussion

Firstly, the equilibrium geometries of bare Al_n^- clusters were optimized first based on the previous calculations. The low-lying isomers of anionic $Al_nS_m^-$ clusters were searched extensively by three ways: 1) by considering the possible structures reported in the previous papers, 2) by placing a S atom at various adsorption or substitution sites on the basis of optimized $Al_nS_{m-1}^-$ geometries, i.e., S-capped, S-substituted and S-concaved patterns, and 3) by placing an Al atom at various adsorption or substitution sites on the basis of optimized $Al_{n-1}S_m^-$ geometries. For the low-lying isomers of neutral species, we also searched them extensively by the same method. Moreover, we used two criteria in comparing the theoretical results with experimental data to select our most likely candidate structures: 1) the relative energies, 2) the vertical detachment energies (VDE) and adiabatic detachment energies (ADE). For the first criterion, only the lowest-energy structures of anionic and neutral Al_nS_m clusters are provided in Figs. 1 and 2, respectively. Meanwhile, symmetries, electronic states and vibration frequencies are listed in Tables 1 and 2. In addition, many low-lying configurations and their corresponding relative energies are shown in Supporting information. For the second criterion, the calculated results and corresponding experimental data are compared at length in the following section.

Equilibrium geometry

The calculated results for Al_2^- show that the quartet spin state is lower in energy than the doublet spin state by

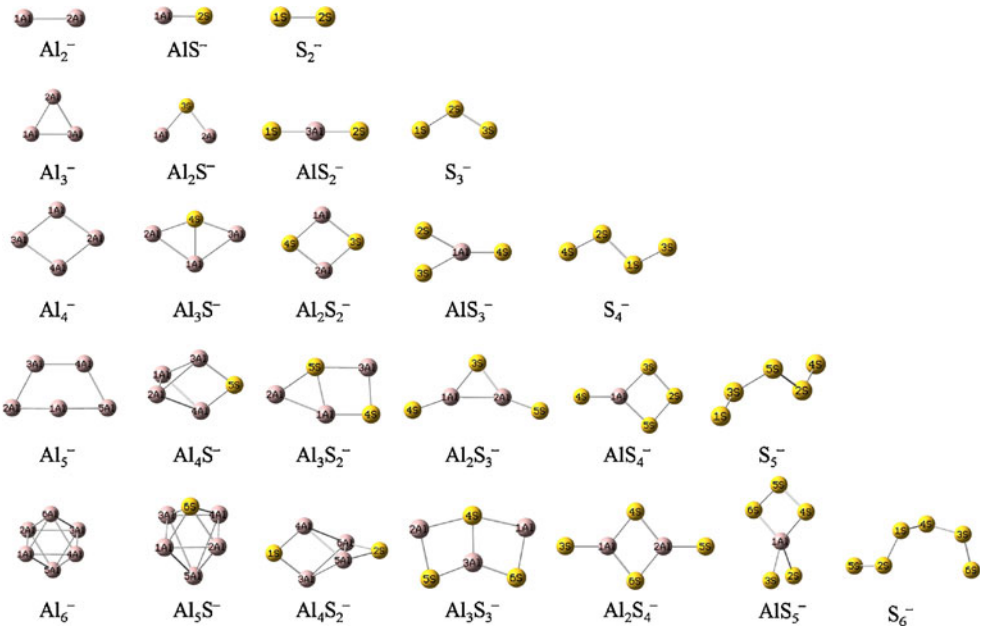

Fig. 1 The lowest-energy structures for the anionic $Al_nS_m^-$ ($n+m\leq6$) clusters

0.74 eV. Equilibrium bond distance of Al_2^- is calculated to be 2.562 Å with $^4\Sigma_g$ symmetry. These results agree well with the previous studies [36–38]. The most stable AlS^- is of $^1\Sigma_g$ symmetry with a bond length of 2.098 Å. The lowest-energy isomer of S_2^- has $^2\Sigma_g$ symmetry and its bond length is 2.003 Å. The optimized geometry of Al_3^- is an equilateral triangle, which has almost equal bond length of 2.513 Å. The present optimized structure of Al_3^- is in good agreement with the previous calculated results [39]. The Al_2S^- geometry with C_{2v} symmetry is optimized as the most stable structure, which is formed by replacing an Al atom on the apex of the equilateral triangle. After that, the lowest-energy isomer turns out to be an acute-angle triangular structure with $^1A_1$ electronic state, a 77° angle and 2.275 Å of Al-S bonds. For AlS_2^-, the most stable isomer is a linear configuration with an Al atom at the center, and 2.056 Å of Al-S bonds. For S_3^- cluster, an obtuse-angle triangular structure is found to be the most stable structure, with a 116° angle and 1.993 Å of S-S bonds. According to the calculated results, it is worth pointing out the bond distances of Al-S have a decreasing tendency with the number of S atoms increasing.

For Al_4^-, the rhombus isomer is found as the lowest-energy structure with equal bond lengths of 2.539 Å and bond angles of 74°. As to Al_3S^-, a planar fanlike isomer is found to be the lowest-energy structure. This structure with

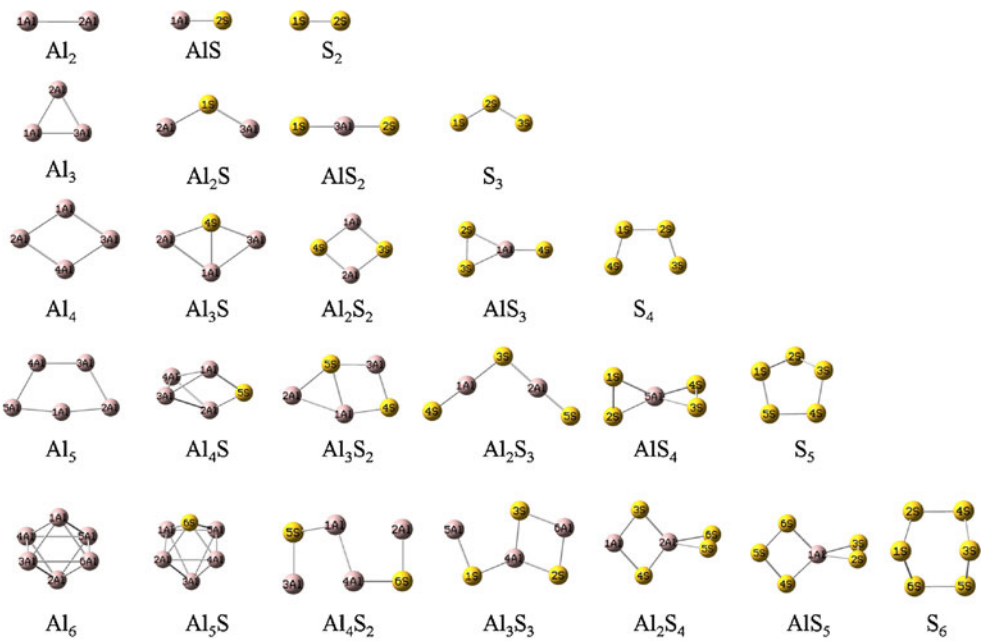

Fig. 2 The lowest-energy structures for the neutral Al_nS_m ($n+m\leq6$) clusters

Table 1 Symmetries, electronic states, HOMO and LUMO energies (au), and vibration frequencies (cm^{-1}) of the lowest-energy $Al_nS_m^-$ clusters

Isomer	Symm.	State	HOMO	LUMO	Frequency
Al_2^-	$D_{\infty h}$	$^4\Sigma_g$	−0.14014	−0.10826	324
AlS^-	$C_{\infty v}$	$^1\Sigma_g$	−0.02520	0.11520	569
S_2^-	$D_{\infty h}$	$^2\Sigma_g$	0.01222	0.08153	592
Al_3^-	D_{3h}	$^1A_1$	−0.01124	0.04648	242, 243, 369
Al_2S^-	C_{2v}	$^2A_1$	0.00848	0.07898	185, 325, 445
AlS_2^-	$D_{\infty h}$	$^1\Sigma_g$	−0.07323	0.09823	176, 176, 427, 757,
S_3^-	C_{2v}	$^2B_1$	−0.02101	0.05739	229, 540, 583
Al_4^-	D_{2h}	^2A_g	−0.02612	−0.03143	87, 158, 274, 275, 317, 336,
Al_3S^-	C_{2v}	$^1A_1$	−0.00501	0.06316	70, 175, 260, 274, 355, 369
$Al_2S_2^-$	D_{2h}	$^2B_{2u}$	−0.02047	0.04206	104, 171, 260, 349, 430, 460,
AlS_3^-	C_{2v}	$^1A_1$	−0.06748	0.08058	152, 179, 331, 366, 464, 716
S_4^-	C_{2h}	^2B_g	−0.03875	0.02788	59, 110, 202, 462, 564, 589
Al_5^-	C_s	$^1A'$	−0.03103	−0.01955	19, 76, 110, 191, 252, 270, 317, 366, 377
Al_4S^-	C_2	^2A	−0.02033	0.04393	47, 78, 88, 144, 214, 279, 339, 350, 477
$Al_3S_2^-$	C_s	^1A	−0.04233	0.05329	42, 93, 147, 181, 237, 265, 361, 393, 502
$Al_2S_3^-$	C_{2v}	$^2A_1$	−0.07752	−0.00130	83, 103, 130, 162, 223, 316, 424, 650, 695
AlS_4^-	C_{2v}	^1A	−0.06692	0.06490	81, 129, 178, 228, 374, 411, 479, 496, 671
S_5^-	C_2	^2A	−0.05997	0.00111	46, 48, 138, 162, 226, 355, 456, 565, 585
Al_6^-	D_{3d}	^2A	−0.04870	0.00885	83, 84, 166, 216, 231, 232, 256, 277, 277, 283, 283, 342
Al_5S^-	C_s	^1A	−0.03567	0.03975	23, 60, 125, 190, 190, 245, 271, 294, 314, 316, 344, 384
$Al_4S_2^-$	C_{2v}	^2A	−0.04702	0.01257	90, 103, 104, 116, 132, 178, 245, 252, 304, 356, 464, 480,
$Al_3S_3^-$	C_{2v}	^1A	−0.05422	0.06716	41, 61, 144, 206, 210, 214, 220, 320, 338, 388, 514, 623
$Al_2S_4^-$	D_{2h}	$^2A'$	−0.12280	−0.06167	47, 88, 138, 177, 208, 223, 311, 399, 400, 489, 527, 639
AlS_5^-	C_{2v}	$^1A'$	−0.06247	0.06496	39, 55, 129, 148, 197, 345, 368, 423, 442, 481, 499, 606
S_6^-	C_1	^2A	−0.07503	−0.01444	30, 56, 68, 130, 172, 230, 249, 296, 446, 464, 565, 580

C_{2v} symmetry and different Al-S bonds (2.355 Å and 2.385 Å) is obtained when the Al atom is added to the most stable Al_2S^- isomer. The Y-shaped structure is found to be the most stable isomer of AlS_3^-, with the Al-S bonds of 2.055 and 2.207 Å as well as the S-S bond of 2.194 Å. For S_4^-, the zigzag structure is a favorable configuration with C_{2h} symmetry. The lowest-energy structures of $Al_nS_m^-$ ($n+m=5$) clusters start to emerge the three-dimensional (3D) structures. As to Al_5^-, according to our calculations, the planar structure with C_{2v} symmetry [39] turns into a slightly distorted 3D structure with C_s symmetry after optimized. For Al_4S^-, the 3D structure with C_2 symmetry is a favorable structure in energy. As to S_5^-, the zigzag structure is still the favorite configuration. For the hexamers, the lowest-energy structures are mostly 3D structures. The octahedral geometry with D_{3d} symmetry is calculated to be the most stable isomer of Al_6^-. It is interesting that the lowest-energy Al_5S^- cluster is optimized after one S atom replacing a top Al atom on the D_{3d} Al_6^- structure. The S-substituted octahedron structure becomes distorted and thus more compact, with a low C_s symmetry. As to AlS_5^-, the optimized most stable structure is formed by attaching other S atom to the Al atom of the AlS_4^- cluster. As the effect of one more S atom, the structure is not planar anymore. The zigzag chain structure is still a favorite isomer of S_6^- cluster energetically.

Equilibrium bond length of Al_2 is calculated to be 2.737 Å with $^3\Sigma_g$ spin state. The most stable AlS cluster is of $^2\Sigma_g$ spin state with bond length of 2.034 Å. The optimized S_2 cluster is of $^3\Sigma_g$ symmetry. The length of S-S bond (1.891 Å) found in this calculation is very close to that of experimental result (1.892 Å) [40]. Furthermore, the calculated bond energy of the Al_2 cluster (1.49 eV) is the smallest, and that of the AlS cluster (6.02 eV) is smaller than that of the S_2 cluster (8.21 eV), calculated for the dissociation to the Al and S atom. It is indicated that the S-S bond is the strongest among them, and the Al-S bond is stronger than the Al-Al bond. For the neutral trimers, the lowest-energy configurations strongly resemble the most stable anionic ones. The optimized Al_3 cluster is still an equilateral triangle, and agrees well with the previous studies [39]. The calculated lowest-energy S_3 isomer is a bent chain with C_{2v} symmetry and the electronic state is singlet $^1A_1$. The length of the S-S bond is 1.910 Å, which is close to the

Table 2 Symmetries, electronic states, HOMO and LUMO energies (au), and vibration frequencies (cm^{-1}) of the lowest-energy Al_nS_m clusters

Isomer	Symm.	State	HOMO	LUMO	Frequency
Al_2	$D_{\infty h}$	$^3\Sigma_g$	−0.16239	−0.10072	269
AlS	$C_{\infty v}$	$^2\Sigma_g$	−0.25888	−0.16505	619
S_2	$D_{\infty h}$	$^3\Sigma_g$	−0.25307	−0.14095	738
Al_3	D_{3h}	$^2A_1'$	−0.17951	−0.11680	242, 242, 362
Al_2S	C_{2v}	$^1A_1$	−0.22149	−0.07345	77, 404, 464
AlS_2	$D_{\infty h}$	$^2\Sigma$	−0.28402	−0.22011	124, 144, 421, 586
S_3	C_{2v}	$^1A_1$	−0.27386	−0.16759	266, 614, 712
Al_4	C_{2h}	^3A_g	−0.18934	−0.13237	54, 184, 218, 296, 310, 333
Al_3S	C_{2v}	$^2B_2$	−0.18068	−0.11242	65, 169, 199, 258, 343, 361
Al_2S_2	D_{2h}	^1A_g	−0.21981	−0.14131	175, 253, 307, 414, 479, 533
AlS_3	C_{2v}	$^2A_2$	−0.23747	−0.20254	121, 125, 269, 323, 585, 740
S_4	C_{2v}	$^1A_1$	−0.24801	−0.16178	109, 217, 339, 392, 669, 698
Al_5	C_{2v}	$^2B_2$	−0.19031	−0.12314	32, 91, 121, 185, 234, 260, 298,391, 392
Al_4S	C_2	^1A	−0.18670	−0.12758	90, 94, 108, 240, 263, 275, 313, 374, 509
Al_3S_2	C_s	^2A	−0.20547	−0.12370	43, 110, 127, 179, 257, 317, 411, 434, 512
Al_2S_3	C_{2v}	$^1A_1$	−0.26920	−0.12373	39, 108, 123, 146, 178, 373, 402, 750, 762,
AlS_4	C_2	^2A	−0.25292	−0.18974	97, 116, 116, 284, 299, 386, 386, 521, 673
S_5	C_s	$^1A'$	−0.23595	−0.09529	92, 238, 290, 302, 351, 353, 445, 522, 530,
Al_6	D_{3d}	$^1A_{1g}$	−0.19342	−0.13331	91, 91, 122, 200, 200, 219, 224, 293, 293, 294, 294, 349
Al_5S	C_s	$^2A'$	−0.19095	−0.11524	50, 78, 144, 206, 215, 257, 266, 288, 307, 308, 328, 392
Al_4S_2	C_2	^1A	−0.20599	−0.11638	31, 71, 80, 128, 160, 171, 213, 280, 356, 361, 502, 504
Al_3S_3	C_s	^2A	−0.22187	−0.13192	37, 47, 83, 159, 203, 252, 366, 373, 394, 436, 532, 619
Al_2S_4	C_{2v}	^3A	−0.22428	−0.17763	75, 83, 109, 177, 211, 285, 354, 406, 441, 540, 544, 611
AlS_5	C_{2v}	^2A	−0.23154	0.18579	44, 77, 104, 136, 198, 267, 324, 379, 454, 507, 522, 608
S_6	C_{2v}	^1A	−0.24243	−0.10956	46, 187, 209, 213, 238, 321, 333, 394, 446, 456, 515, 526

previous precise results (1.917 Å) [41]. The angle (118.5°) is within 2° of that for the isovalent molecules O_3 (116.8°), SO_2 (119.5°) and S_2O (118°), indicating sp^2 hybridization for the apex sulfur atom [42]. The separation between the terminal S atoms (3.284 Å) agrees fairly well with Van der Waals distance between S atoms in the solid allotropes, confirming that S_3 is best described as a bent chain rather than a three-membered ring (Supporting information).

The optimized geometry of Al_4 is triplet ^3A_g state, with C_{2h} symmetry, while the previous reported structure with D_{2h} symmetry [39] has one imaginary frequency in our calculation. For the neutral tetramer, the lowest-energy structures strongly resemble their anionic lowest-energy configuration except S_4 cluster. Our calculations favor the singlet planar trapezoidal structure with C_{2v} symmetry. A zigzag structure with C_{2h} symmetry is calculated to lie at 0.24 eV higher in energy. The length of the terminal bond found in this way (1.901 Å) is close to that of S_2 (1.892 Å) [40], while the central bond (2.094 Å) is qualitatively similar to that in S_2O_2, a molecule of similar structure [43]. The S-S-S angle yielded values in the range 106°–112° with different methods, consistent with the 106° characteristic of many sulfur rings [44]. The angle derived here (107°) is highly reasonable in this range.

The favorable geometry of Al_5 cluster is a planar structure with C_{2v} symmetry and doublet $^2B_2$ spin state. The 3D structure of Al_4S cluster with C_2 symmetry is similar to its anionic lowest-energy structure. The planar geometry of Al_3S_2 still keeps an analogous structure of $Al_3S_2^-$ cluster. The V-shaped geometry with C_{2v} symmetry is calculated to be the lowest-energy structure of Al_2S_3. The most stable AlS_4 cluster is a doublet nonplanar structure with C_2 symmetry. The five-membered ring structure is reported to be the lowest-energy S_5 isomer, with $^1A'$ spin state, which is consistent with the previous predictions [41].

The octahedral structure with D_{3d} symmetry is calculated to be the lowest-energy Al_6 cluster, which is in agreement with the published results [39]. For the Al_5S cluster, the most stable isomer bears a strong resemblance to the anionic lowest-energy one. The inverted S-shaped geometry with C_2 symmetry is the lowest-energy Al_4S_2 isomer. The distorted book-shaped structure is the favorable geometry of Al_3S_3. For the Al_2S_4 cluster, the most stable isomer with C_{2v} symmetry has the triplet spin state. This geometry can be viewed as two S

atoms capped on the same Al atom of the most stable Al_2S_2 cluster, and the bond length of two S atoms is 2.023 Å. Our calculation favors the doublet structure with C_{2v} symmetry, which is similar to its corresponding anionic most stable Al_5S^- cluster. The S-S bond length is 2.066 Å in this structure. For S_6, the ring structure is still the most stable isomer, which is in agreement with the previous predictions [41].

According to the above discussion, the most stable isomers are 2D structures for the anionic and neutral Al_nS_m ($n+m\leq4$) clusters, and their geometries are analogous to each other, while the 3D structures are favorable structures for most of anionic and neutral Al_nS_m ($5\leq n+m\leq6$) clusters. The low (singlet or doublet) spin states are preferable for the anionic and neutral most stable Al_nS_m ($2\leq n+m\leq6$) clusters except for the Al_2^-, Al_2, S_2, Al_4 and Al_2S_4 clusters. The bond length of Al-S decreases with the increase in number of S atoms. This may be caused by clusters with large sulfur atomic numbers having stronger interactions.

HOMO-LUMO energy gap

The electronic properties of cluster can be reflected by the highest occupied-lowest unoccupied molecular orbital (HOMO-LUMO) energy gaps, VDE, ADE, VIP, VEA and chemical hardness. Among them, the HOMO-LUMO gap is considered to be an important criterion in terms of the electronic stability of clusters [45]. It represents the ability of a molecule to participate in a chemical reaction to some degree. A large value of the HOMO-LUMO energy gap is related to an enhanced chemical stability. For the lowest-energy $Al_nS_m^-$ clusters, HOMO and LUMO energies at each cluster size are listed in Table 1. Meanwhile, the size dependence of the HOMO-LUMO gaps is shown in Fig. 3. It is noted that the HOMO-LUMO energy gaps present pronounced odd-even oscillatory behaviors for the series of $n+m=2$, $n+m=4$ and $n+m=6$. This indicates that AlS^-, Al_3S^-, AlS_3^-, Al_5S^-, $Al_3S_3^-$ and AlS_5^- clusters with odd-number sulfur atoms have larger HOMO-LUMO energy gaps than their vicinity clusters. Namely, they are relatively weaker in chemical activity than those with an even-number of sulfur atoms. However, the HOMO-LUMO energy gaps exhibit inverse odd-even oscillations for the series of $n+m=3$ and $n+m=5$ (except for Al_3^- and Al_5^-). That is, the AlS_2^-, $Al_3S_2^-$ and AlS_4^- clusters with even-number sulfur atoms have larger HOMO-LUMO energy gaps than their vicinity clusters. Namely, they are less reactive than clusters with odd-number sulfur atoms. Furthermore, all clusters with large HOMO-LUMO energy gaps are checked that they have closed shell electron configurations, which always play an important role in the dramatically enhanced chemical stability. Specifically, it is found that the top largest HOMO-LUMO energy gaps of 4.67, 4.03, 3.82, 3.59 and 3.47 eV are found for the lowest-energy AlS_2^-, AlS_3^-, AlS^-, AlS_4^- and AlS_5^- clusters, respectively. All these clusters have only one Al atom.

Vertical and adiabatic electron detachment energy

Experimentally, anion photoelectron spectra (PES) were reported for Al_nS^- by Nakajina et al. [17]. It was found that the electron detachment energy increased monotonically from $n=2$ to 5. Moreover, the photoelectron spectra of $Al_nS_m^-$ clusters were measured using a magnetic-bottle photoelectron apparatus equipped with a laser vaporization cluster source [18]. In order to implement the second criterion, we discuss the adiabatic and vertical detachment energies (ADE and VDE) as compared with experimental values in Table 3. Meanwhile, the variation trends of the ADE and VDE for the Al_nS_m clusters with different cluster size are plotted in Fig. 4. VDE is defined as the energy difference between the neutral clusters at optimized anion geometry clusters and optimized anion clusters.

$$\mathrm{VDE} = \mathrm{E}_{(\text{neutral at optimized anion geometry})} - \mathrm{E}_{(\text{optimized anion})} \quad (1)$$

To calculate the ADE of the most stable Al_nS_m clusters, we check the energy difference between the optimized anion geometry and the optimized neutral geometry. This quantity can also be referred to as the adiabatic electron affinity. So, ADE is studied by the following formula:

$$\mathrm{ADE} = \mathrm{E}_{(\text{optimized neutral})} - \mathrm{E}_{(\text{optimized anion})}. \quad (2)$$

Cha et al. [46] and Li et al. [47] have studied the VDE of the Al_n clusters in order of priority. Their results are in agreement with each other. So, only Li's results are listed in the Table 3. Our VDE results are in good agreement with the experimental results [47]. The calculated ADE results are all appreciably overestimated, but the trend is in good agreement with the experiments [48] and theory [36]. It is worth pointing out the VDE and ADE increase monotonically with the number of Al atoms ($n\leq6$). For the lowest-energy structure of $Al_{2\text{-}4}^-$, our VDE at B3PW91/6-311+G (3df) level (1.58, 1.71 and 2.17 eV) are in good agreement with the experimental data from Cha et al. [49] for Al_2^- (1.60 eV), Al_3^- (1.90 eV) and Al_4^- (2.20 eV) as well as those from Li et al. [50] for Al_2^- (1.46±0.01 eV), Al_3^- (1.89±0.04 eV) and Al_4^- (2.20±0.05 eV). Only Al_3^- (1.71 eV) is lower than the experimental values. For $Al_{5\text{-}6}^-$ the calculated VDE at B3PW91/6-311+G (3df) level are 2.17 and 2.62 eV consistent with the experimental data for Al_5^- (2.25±0.05 eV) and Al_6^- (2.63±0.06 eV).

Photoelectron spectra of Al_nS^- cluster anions were measured at the photo energies of 3.49 and 4.66 eV, using a magnetic bottle time of flight (TOF) spectrometer having

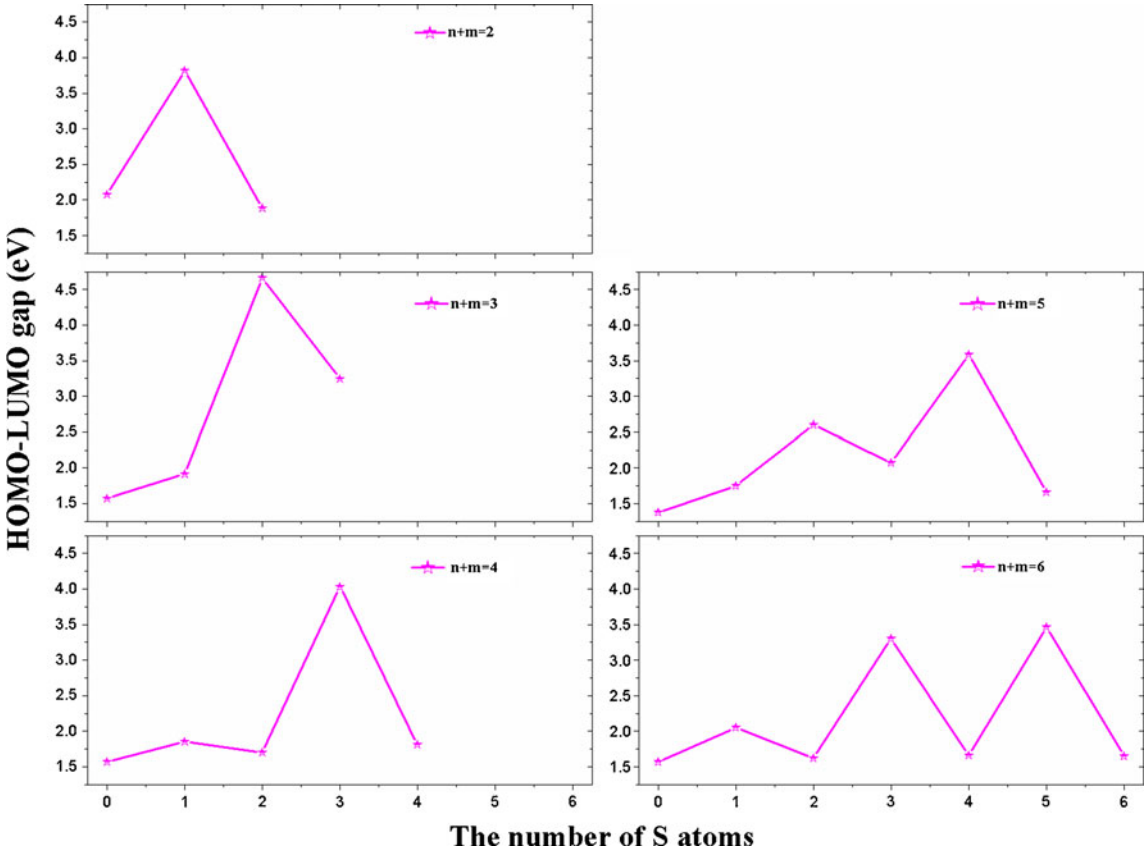

Fig. 3 The HOMO-LUMO energy gaps for anionic $Al_nS_m^-$ ($n+m\leq6$) clusters *versus* the number of S atoms

~60 meV resolutions [17]. Our calculated VDE of the lowest-energy Al_nS^- ($1\leq n\leq5$) clusters are 2.63, 1.39, 1.60, 2.07 and 2.35 eV, respectively, consistent with 7the experimental data for AlS^- (2.75±0.04 eV), Al_2S^- (1.16±0.05 eV), Al_3S^- (1.64±0.06 eV), Al_4S^- (1.96± 0.08 eV) and Al_5S^- (2.46±0.06 eV) [17]. The ADE at the same level are 2.59, 1.15, 1.59, 2.04 and 2.10 eV for the Al_nS^- ($1\leq n\leq5$) clusters, respectively, in good agreement with the experimental results for AlS^- (2.60±0.03 eV), Al_2S^- (0.80±0.12 eV), Al_3S^- (1.52±0.12 eV), Al_4S^- (1.83±0.06 eV) and Al_5S^- (2.17±0.08 eV). The ADE and VDE monotonically increased for Al_nS^- ($2\leq n\leq5$) clusters. AlS^- had an ADE of as large as 2.6 eV, attributed to large stability by six bonding electrons. For Al_4S^-, the VDE and ADE are more close to Zhang et al.'s results, 2.01 and 1.96 eV, respectively. By the same method of Al_nS^- clusters, the photoelectron spectra of $Al_nS_m^-$ cluster anions were also measured. For the most stable $Al_nS_2^-$ ($1\leq n\leq4$) clusters, our calculated VDE are 3.98, 2.28, 2.73 and 2.72 eV, respectively, consistent with the experimental data for $Al_2S_2^-$ (2.14±0.11 eV), $Al_3S_2^-$ (2.93±0.06 eV) and $Al_4S_2^-$ (2.77±0.06 eV) [18]. Meanwhile, the ADE are 3.97, 2.19, 2.35 and 2.22 eV, respectively, in good agreement with the experimental results for $Al_2S_2^-$ (1.90± 0.06 eV), $Al_3S_2^-$ (2.49±0.14 eV) and $Al_4S_2^-$ (2.20± 0.09 eV) [18]. For AlS_2^-, no photoelectrons are observed even with the 266 nm detachment, since the ADE of AlS_2^- is very large. From the viewpoint of stoichiometry, Al and S atoms take a valence of +3 and −2, respectively, so that the valence is strictly satisfied in AlS_2^-. The high ADE of AlS_2^- is seemingly attributed to the complete valence. It is worth pointing out the even-odd alternation phenomenon in electron detachment energies with the cluster size are found in the series of Al_nS_2 ($1\leq n\leq4$) clusters.

Unfortunately, there are no available experimental data that can provide direct information for the S_m^- ($2\leq m\leq6$), AlS_m^- ($1\leq m\leq5$) and $Al_2S_m^-$ ($1\leq m\leq4$) clusters. Although, no photoelectrons are observed with 355 nm detachment for $Al_2S_3^-$, a extraordinary large ADE has been predicted in the weak spectra at 266 nm [18]. However, the stoichiometry predicts that the ADE of $Al_2S_3^-$ should be small, because the valence is completely satisfied in neutral Al_2S_3 but not in anionic $Al_2S_3^-$. According to our calculation $Al_2S_3^-$ takes a structure of $(AlS_2\text{-}AlS)^-$, where the high electron binding energy is attributed to the partial structure of AlS_2^- in the cluster. For all clusters, it is noted that ADE are smaller than VDE. Some calculated values of the ADE and VDE are very close, perhaps because of their highly similar structures, while others are remarkably separated perhaps due to the large discrepancy in the most stable anionic and neutral structures.

Table 3 Electron detachment energies (adiabatic ADE and vertical VDE), vertical electron affinity (VEA), vertical ionization potential (VIP) and chemical hardness η (eV) of the lowest-energy Al_nS_m clusters

Isomer	ADE	Expt.	VDE	Expt.	VEA	VIP	η
Al_2	1.52		1.58	1.46(1)[47]	1.17	6.08	4.91
AlS	2.59	2.60(3)[17]	2.63	2.75(4)[17]	2.55	9.29	6.74
S_2	2.64		2.80		2.49	8.67	6.18
Al_3	1.69	1.53[48]	1.71	1.89(4)[47]	1.71	6.77	5.06
Al_2S	1.15	0.80(12)[17]	1.39	1.16(5)[17]	0.55	7.90	7.35
AlS_2	3.97		3.98		3.96	9.70	5.74
S_3	2.53		2.70		2.36	9.80	7.44
Al_4	1.81	1.74[48]	2.17	2.20(5)[47]	1.95	6.60	4.65
Al_3S	1.59	1.52(12)[17]	1.60	1.64(6)[17]	1.56	6.63	5.07
Al_2S_2	2.19	1.90(6)[18]	2.28	2.14(11)[18]	2.09	7.74	5.65
AlS_3	3.66		3.96		3.38	8.63	5.25
S_4	2.54		2.98		2.36	8.81	6.45
Al_5	2.09	1.82[48]	2.17	2.25(5)[47]	2.02	6.47	4.45
Al_4S	2.04	1.96[19]	2.07	2.01[19]	1.99	6.60	4.61
Al_3S_2	2.35	2.49(14)[18]	2.73	2.93(6)[18]	1.89	7.55	5.66
Al_2S_3	3.01		3.83		1.87	9.04	7.17
AlS_4	3.42		3.61		3.28	8.83	5.55
S_5	2.09		2.98		0.69	8.45	7.76
Al_6	2.25	2.09[48]	2.62	2.63(6)[47]	2.22	6.61	4.39
Al_5S	2.10	2.17(8)[17]	2.35	2.46(6)[17]	1.77	6.75	4.98
Al_4S_2	2.22	2.20(9)[18]	2.72	2.77(6)[18]	1.76	7.08	5.32
Al_3S_3	2.68	3.01(10)[18]	2.98	3.20(6)[18]	2.12	7.79	5.67
Al_2S_4	3.96		4.38		2.80	8.05	5.25
AlS_5	3.37		3.99		3.20	8.56	5.36
S_6	2.38		3.20		1.22	8.51	7.29

Vertical ionization potential, vertical electron affinity and chemical hardness

In cluster science, vertical ionization potential (VIP) and vertical electron affinity (VEA) are the most important characteristics reflecting the size-dependent relationship of electronic structure. In this section, the VIP and VEA can be defined as the following:

$$\mathrm{VIP} = \mathrm{E}_{(\text{cation at optimized neutral geometry})} - \mathrm{E}_{(\text{optimized neutral})} \quad (3)$$

$$\mathrm{VEA} = \mathrm{E}_{(\text{optimized neutral})} - \mathrm{E}_{(\text{anion at optimized neutral geometry})} \quad (4)$$

Next, we have calculated the VIP and VEA of the Al_nS_m clusters. The calculated results are listed in Table 3 and the variation trends of VIP related to the sulfur atoms are shown as a function of cluster size in Fig. 5. It can be seen from Fig. 5, VIP of the Al_nS_m ($n+m$=3, 4 and 6) clusters have smooth increasing trends with the number of S atoms. For the series of $n+m$=2 and 5, the local peaks appear at AlS and Al_2S_3, respectively. The clusters with high VIP have electronic stabilities.

Chemical hardness η has been established as an electronic quantity which may be applied in characterizing the relative stability of molecules and aggregate through the principle of maximum hardness proposed by Pearson [49]. On the basis of a finite difference approximation and the Koopmans theorem [50], the chemical hardness η is expressed as:

$$\eta = \mathrm{I} - \mathrm{EA}, \quad (5)$$

where I is the vertical ionization potential (VIP) and EA is vertical electron affinity (VEA) [51, 52]. In Table 3, we list the calculated results of the chemical hardness for Al_nS_m clusters. The relationships of hardness with the number of S atoms are plotted in Fig. 5. From Fig. 5, it is found that the variation trend of η is in keeping with that of HOMO-LUMO gaps, indicating the chemical hardness η or the stability is closely associated with the frontier orbitals. Especially, the oscillating behaviors exhibit in the series of $n+m$=2, 3, 4 and 5.

Interaction of AlS_m^- clusters with O_2

Understanding the catalytic of aluminum sulfides at the molecular level can help design better catalysts. Interaction of gas-

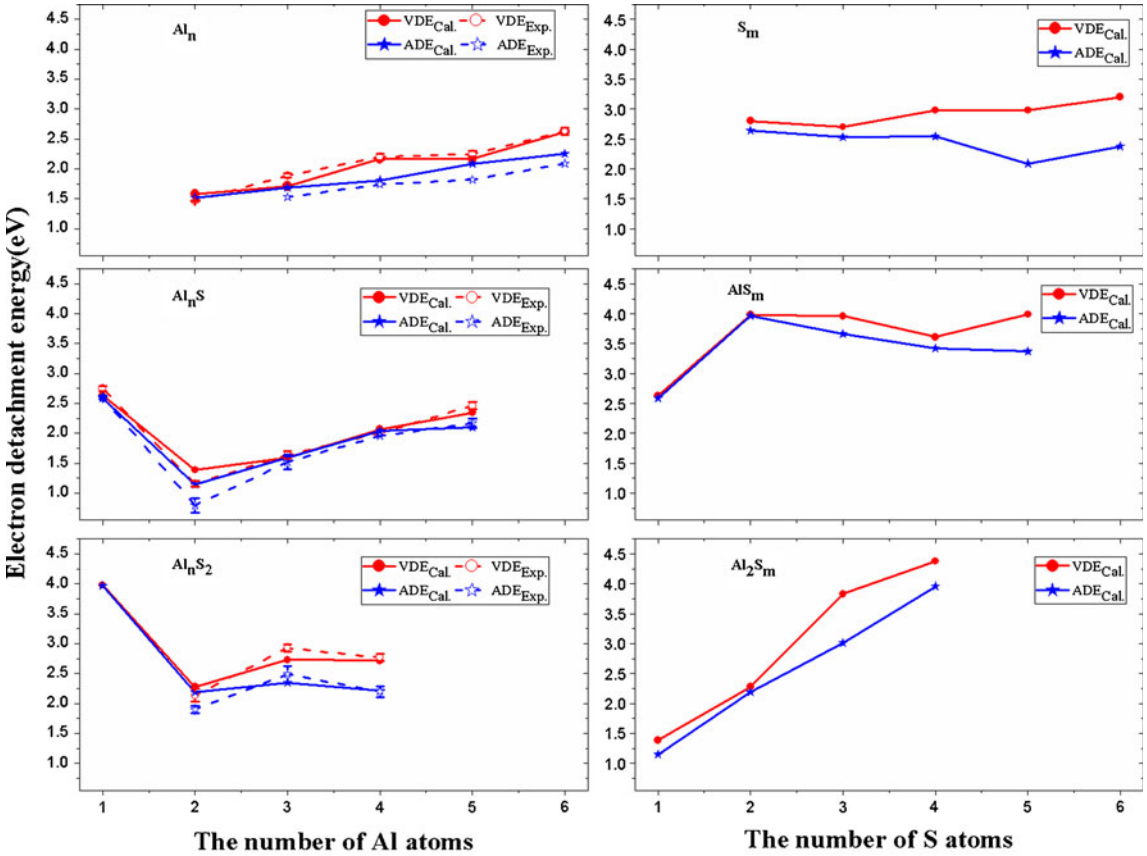

Fig. 4 Calculated and experimental adiabatic (ADE) and vertical (VDE) detachment energies for the lowest-energy Al_nS_m clusters *versus* the number of Al and S atoms

phase cluster with small molecule studies can provide valuable structural models and mechanistic information for real world catalysis. In order to understand the fundamentally important oxidation of metal sulfide nanoparticles, we have performed the interaction of oxygen with stable Al-S systems. Here, we only study AlS_m^- ($1 \le m \le 5$) clusters, because they are found to have significantly large HOMO-LUMO energy gaps. We have preformed the geometry optimization of $AlS_mO_2^-$ complexes, by keeping the molecular identity of oxygen. Meanwhile, the calculated lowest-energy structures are shown in Fig. 6. On account of the optimized most stable structures of $AlS_mO_2^-$ complexes, we report the binding energy calculated as:

$$E_b = E(O_2) + E(AlS_m^-) - E(AlS_mO_2^-). \quad (6)$$

Here, $E(O_2)$, $E(AlS_m^-)$ and $E(AlS_mO_2^-)$ represent the total energies of the O_2 molecule, the most stable bare and complex clusters, respectively. The thermodynamic quantity like Gibbs free energy (G) is studied at a pressure of 1 atm and a temperature of 298.17 K using the ideal gas approximation. The calculation of the change in Gibbs free energy (ΔG) is necessary to confirm whether adsorption is thermodynamically favorable or not. If the ΔG is negative then the adsorption is thermodynamically favorable.

We have optimized large initial configurations keeping O_2 in different orientations with respect to the AlS^-. The results show that when O_2 approaches Al, it is favorable in energy, and remains in the molecular form with the O-O bond length of 1.408 Å (in Table 4). For the $AlS_2O_2^-$ complex, it is observed after the geometry optimized that molecular oxygen dissociates into its atomic form. That is one oxygen atom is connected to Al atom and the other to S atom, and the interoxygen distance is estimated to increase to 1.457 Å. Dissociative adsorption is predicted to induce large distortion of the bare cluster. The similar dissociative adsorptions emerge in the $AlS_3O_2^-$ and $AlS_4O_2^-$ complexes, and induce the Al-S systems into 3D structures. Especially for $AlS_5O_2^-$, the former Al-S bond has been broken and forms a five-membered ring, in which the O-O bond length is 1.465 Å. The calculated binding energy and Gibbs free energy change of $AlS_mO_2^-$ ($1 \le m \le 5$) complexes for the lowest-energy structures are summarized in Table 4. At the same time, the corresponding variations of E_b and ΔG with the cluster size are shown in Fig. 6. As can be seen in Fig. 6, the binding energy shows obvious oscillating behaviors as the cluster size increases. However, the Gibbs free energy change exhibits diametrically opposite oscillating behaviors. It indicates that the complexes at m=1, 3 and 5

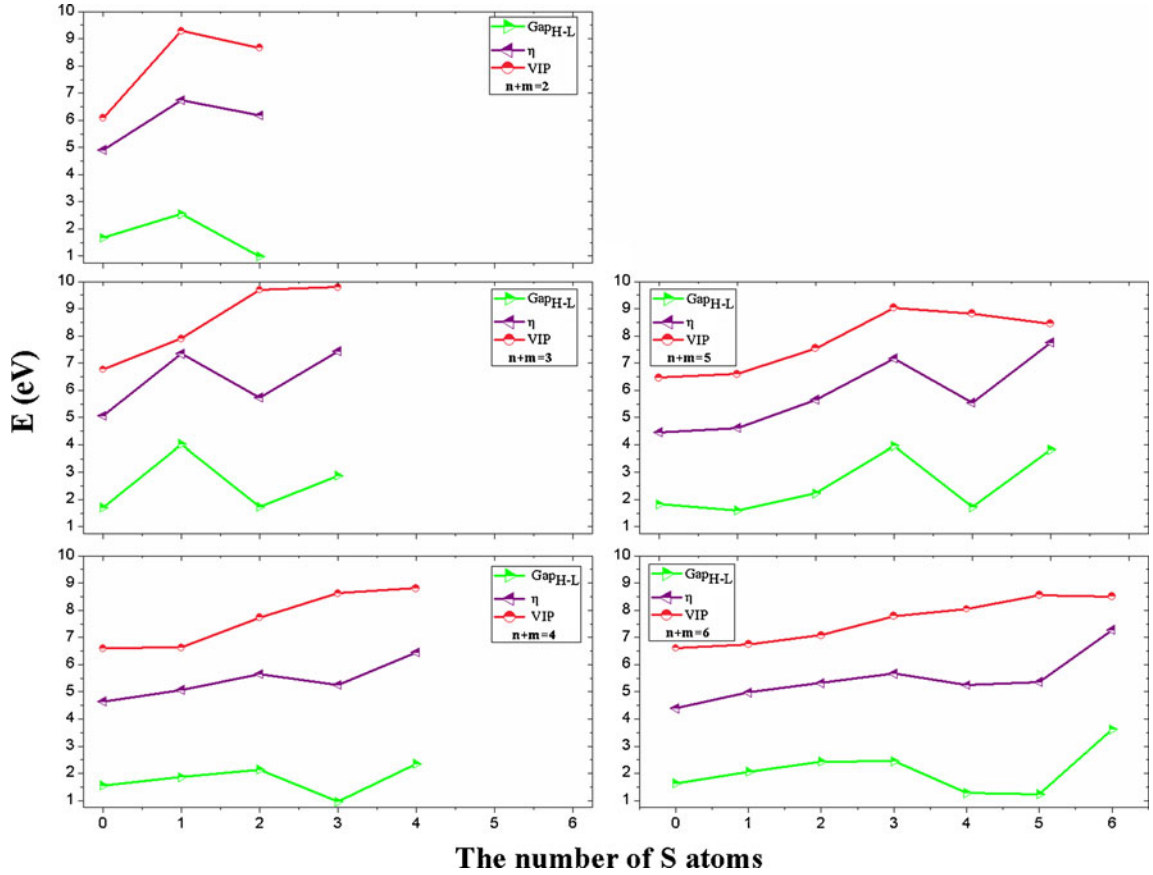

Fig. 5 The HOMO-LUMO energy gaps and vertical ionization potential (VIP) and chemical hardness η for the lowest-energy Al_nS_m clusters *versus* the number of S atoms

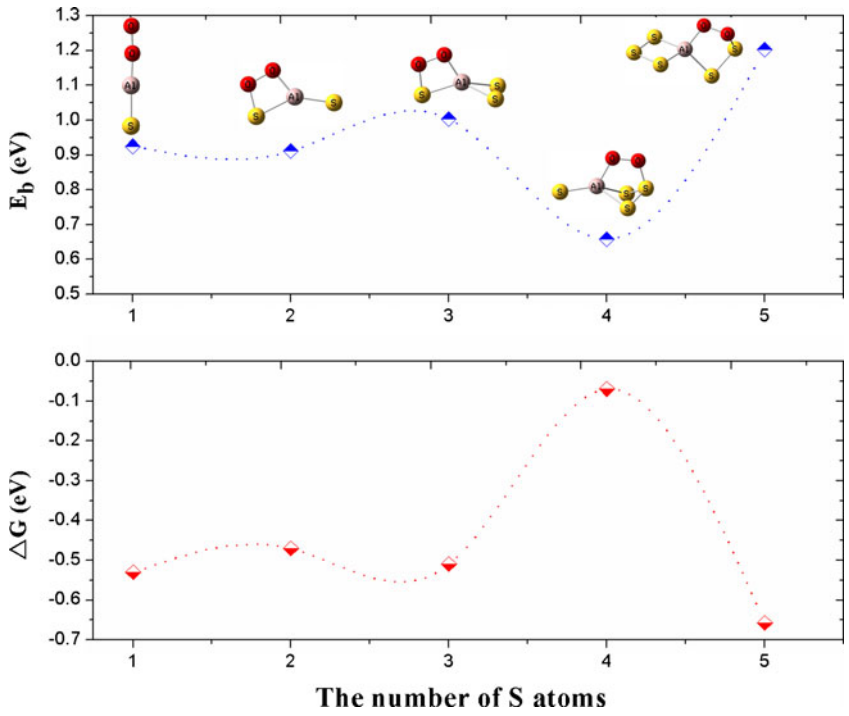

Fig. 6 Calculated binding energy (E_b) and Gibbs free energy change (ΔG) for the lowest-energy $AlS_mO_2^-$ clusters *versus* the number of S atoms

Table 4 The O-O bond distances R_{O-O} (Å), electronic states, the highest vibrational frequencies (cm^{-1}), binding energies E_b and Gibbs free energy changes ΔG (eV) of the lowest-energy $AlS_mO_2^-$ clusters

Isomer	$AlSO_2^-$	$AlS_2O_2^-$	$AlS_3O_2^-$	$AlS_4O_2^-$	$AlS_5O_2^-$
R_{O-O}	1.408	1.457	1.460	1.433	1.465
State	^1A	^1A	^1A	^1A	^1A
Frequency	1197	886	894	868	810
E_b	0.93	0.91	1.00	0.66	1.20
ΔG	−0.53	−0.47	−0.51	−0.07	−0.66

with higher E_b and more negative ΔG are more stable than their neighboring complexes after oxygen adsorption. It is noteworthy that all ΔG are negative, indicating that these adsorption are thermodynamically favorable.

Conclusions

A detailed study on the geometric structures and electronic properties including the HOMO-LUMO energy gaps, electron detachment energy and chemical hardness of anionic and neutral Al_nS_m ($n+m\leq6$) clusters and the oxidation reaction of the most stable AlS_m^- ($1\leq m\leq5$) clusters has been preformed by DFT calculations realized with the B3PW91/6-311+G(3df) method. The calculated results are summarized as follows:

i) The optimized results indicate the most stable configurations of the anionic and neutral Al_nS_m clusters prefer the low spin multiplicities (singlet or doublet) except the Al_2^-, Al_2, S_2, Al_4 and Al_2S_4 clusters. The Al-S bond length is decreases with the increase in the number of S atoms. The clusters with large sulfur atomic number have stronger interactions.

ii) The highest occupied-lowest unoccupied molecular orbital (HOMO-LUMO) energy gaps exhibit pronounced odd-even oscillatory behaviors for the series of $n+m=2$, 4 and 6, while an inverse oscillations for the series of $n+m=3$ and 5. All the clusters with large HOMO-LUMO energy gaps have closed shell electron configurations which always play an important role in the dramatically enhanced chemical stability. Particularly, the top largest HOMO-LUMO energy gaps of 4.69, 4.03, 3.82, 3.59 and 3.47 eV are found in the series of the lowest-energy AlS_m^- clusters.

iii) The vertical and adiabatic detachment energies (VDE and ADE) are discussed and compared with the experimental observations. The results show good agreement, thereby giving confidence in the most stable clusters considered in the present paper and validating the chosen computational method. However, there are no available experimental results for the $Al_2S_m^-$, AlS_m^- and S_m^- clusters, therefore our theoretical findings may provide a reference for further experimental and theoretical studies. In addition, the variation trend of chemical hardness keeps with that of HOMO-LUMO energy gaps for the Al_nS_m clusters.

iv) We have also performed the interaction of oxygen with the stable AlS_m^- clusters. The results suggest that the adsorption of oxygen favors dissociative chemisorptions mechanism. The binding energy and Gibbs free energy change show completely opposite oscillating behaviors as the cluster size increases.

Acknowledgments This work was supported by the National Natural Science Foundation of China (No. 10974138 and No. 11104190) and the Doctoral Education Fund of Education Ministry of China (No. 20100181110086 and No. 20111223070653).

References

1. Ravaghavachari K (1990) J Chem Phys 93:5862–5874
2. Trost J, Brune H, Wintterlin J, Behm RJ, Ertl G (1998) J Chem Phys 108:1740–1747
3. Wang XB, Niu SQ, Yang X, Ibrahim SK, Pickett CJ, Ichiye T, Wang LS (2003) J Am Chem Soc 125:14072–14081
4. Li X, Kiran B, Cui LF, Wang LS (2005) Phys Rev Lett 95:253401
5. Majumder C, Kandalam AK, Jena P (2006) Phys Rev B 74:205437
6. Ackerson CJ, Jadzinsky PD, Jensen GJ, Kornberg RD (2006) J Am Chem Soc 128:2635–2640
7. Weckhuysen BM, Keller DE (2003) Catal Today 78:25–46
8. El-Nakat JH, Dance IG, Fisher KJ, Rice D, Willett GD (1991) J Am Chem Soc 113:5141–5148
9. El-Nakat JH, Dance IG, Fisher KJ, Willett GD (1991) Inorg Chem 30:957–2958
10. El-Nakat J, Fisher KJ, Dance IG, Willett GD (1993) Inorg Chem 32:1931–1940
11. Dance IG, Fisher KJ, Willett GD (1996) Inorg Chem 35:4177–4184
12. Fisher K, Dance I, Willett G, Yi MN (1996) Dalton Trans 709–718
13. Dance IG, Fisher KJ, Willett GD (1997) Dalton Trans 2557–2561
14. Nakajima A, Hayase T, Hayakawa F, Kaya K (1997) Chem Phys Lett 280:381–389
15. Zhang N, Hayase T, Kawamata H, Nakao K, Nakajima A, Kaya K (1996) J Chem Phys 104:3413–3419
16. Zhang N, Kawamata H, Nakajima A, Kaya K (1996) J Chem Phys 104:36–41
17. Nakajima A, Hayase T, Nakao K, Hoshino K, Iwata S, Kaya K (1995) J Chem Phys 102:660–665
18. Nakajima A, Zhang N, Kawamata H, Hayase T, Nakao K, Kaya K (1995) Chem Phys Lett 241:295–300
19. Zhang ZG, Xu HG, Feng Y, Zheng WJ (2010) J Chem Phys 132:161103
20. Zhang N, Yu ZD, Wu XJ, Gao Z, Zhu QH, Kong FN (1993) Faraday Trans 89:1779–1782
21. Yu ZD, Zhang N, Wu XJ, Gao Z, Zhu QH, Kong FN (1993) J Chem Phys 99:1765–1770
22. Shi Y, Zhang N, Gao Z, Kong FA, Zhu QH (1994) J Chem Phys 101:9528–9533
23. Zhao YC, Yuan JY, Zhang ZG, Xu HG, Zheng WJ (2011) Dalton Trans 40:2502–2508
24. Aizman A, Case DA (1982) J Am Chem Soc 104:3269–3279

25. Noodleman L, Baerends EJ (1984) J Am Chem Soc 106:2316–2327
26. Noodleman L, Case DA (1992) Ad Inorg Chem 38:423–470
27. Noodleman L, Peng CY, Case DA, Mouesca JM (1995) Coord Chem Rev 144:199–244
28. Liang B, Andrews L (2002) J Phys Chem A 106:6295–6301
29. Liang B, Andrews L (2002) J Phys Chem A 106:3738–3743
30. Liang B, Andrews L (2002) J Phys Chem A 106:6945–6951
31. Liang B, Wang X, Andrews L (2009) J Phys Chem A 113:5375–5384
32. Liang B, Wang X, Andrews L (2009) J Phys Chem A 113:3336–3343
33. Frisch MJ, Trucks GW, Schlegel HB, Scuseria GE, Robb MA, Cheeseman JR, Montgomery JJA, Vreven T, Kudin KN, Burant JC, Millam JM, Iyengar SS, Tomasi J, Barone V, Mennucci B, Cossi M, Scalmani G, Rega N, Petersson GA, Nakatsuji H, Hada M, Ehara M, Toyota K, Fukuda R, Hasegawa J, Ishida M, Nakajima T, Honda Y, Kitao O, Nakai H, Klene M, Li X, Knox JE, Hratchian HP, Cross JB, Bakken V, Adamo C, Jaramillo J, Gomperts R, Stratmann RE, Yazyev O, Austin AJ, Cammi R, Pomelli C, Ochterski J, Ayala PY, Morokuma K, Voth GA, Salvador P, Dannenberg JJ, Zakrzewski VG, Dapprich S, Daniels AD, Strain MC, Farkas O, Malick DK, Rabuck AD, Raghavachari K, Foresman JB, Ortiz JV, Cui Q, Baboul AG, Clifford S, Cioslowski J, Stefanov BB, Liu G, Liashenko A, Piskorz P, Komaromi I, Martin RL, Fox DJ, Keith T, Al-Laham MA, Peng CY, Nanayakkara A, Challacombe M, Gill PMW, Johnson BG, Chen W, Wong MW, Gonzalez C, Pople JA (2004) GAUSSIAN 03, Revision E01. Gaussian Inc, Wallingford, CT
34. Becke AD (1993) J Chem Phys 98:5648–5652
35. Perdew JP, Wang Y (1992) Phys Rev B 45:13244–13249
36. Rao BK, Jena P (1999) J Chem Phys 111:1890–1904
37. Zhan CG, Zheng F, Dixon DA (2002) J Am Chem Soc 124:14795–14803
38. Boldyrev AI, Schleyer PVR (1991) J Am Chem Soc 113:9045–9054
39. Sun J, Lu WC, Wang H, Li ZS, Sun CC (2006) J Phys Chem A 110:2729–2738
40. Pickett HM, Boyd TL (1979) J Mol Spectrosc 75:53–57
41. McCanrthy MC, Thorwirth S, Gottlieb CA, Thaddeus P (2004) J Am Chem Soc 126:4096–4097
42. Wiberg N, Holleman A, Wilberg E (eds) (2001) Inorg Chem. Academic, San Diego, p 532
43. Lovas FJ, Tiemann E, Johnson DR (1974) J Chem Phys 60:5005–5010
44. Meyer B (1977) Sulfur, energy, and environment. Elsevier, Amsterdam
45. Sannigrahi AB, Nandi PK, Schleyer PR (1994) J Am Chem Soc 116:225–7232
46. Cha CY, Gantefr G, Eberhardt W (1994) J Chem Phys 100:995–1010
47. Li X, Wu H, Wang XB, Wang LS (1998) Phys Rev Lett 81:1909–1912
48. Taylor KJ, Pettiette CL, Graycraft MJ, Chesnovsky O, Smalley RE (1988) Chem Phys Lett 152:347–352
49. Pearson RG (1997) Chemical hardness: applications from molecules to solids. Wiley-VCH, Weinheim
50. Parr RG, Yang W (1989) Density functional theory of atoms and molecules Oxford. University Press, New York
51. Chermette H (1999) J Comput Chem 20:129–154
52. Senet P (1997) Chem Phys Lett 275:527–532